Full Paper: Aqueous micelles have been prepared from amphiphilic supramolecular graft copolymers, in which poly(ethylene glycol) (PEG) side chains were linked to a poly(methyl methacrylate) (PMMA) backbone via ruthenium(II)-terpyridine complexes. Three different graft copolymers were investigated, in which the average number of PEG branches (constant length) and the length of the PMMA backbone were varied. The successful formation of micelles was proven by dynamic light scattering (DLS), atomic force microscopy (AFM), and transmission electron microscopy (TEM). A good agreement was found between TEM and AFM observations, which show polydisperse spherical micelles. The hydrodynamic diameter measured by DLS was much larger, suggesting the formation of aggregates. No substantial difference in the micellar characteristic features was found between the three investigated samples.

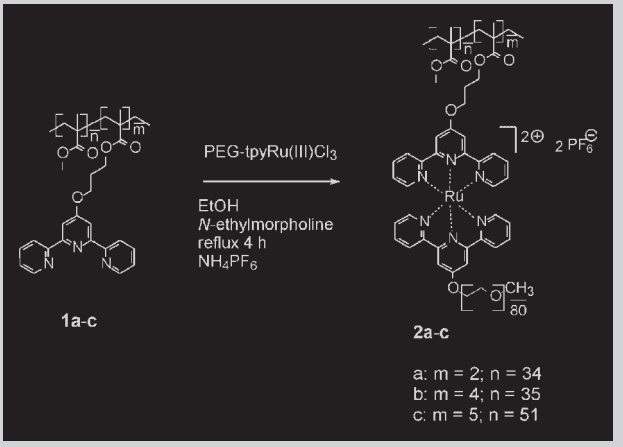

Schematic representation of the graft copolymer synthesis.

Aqueous Micelles from Supramolecular Graft Copolymers

Jean-François Gohy,[1,2] *Harald Hofmeier,*[1,3] *Alexander Alexeev,*[1] *Ulrich S. Schubert**[1,3]

[1] Laboratory of Macromolecular Chemistry and Nanoscience, Eindhoven University of Technology and Dutch Polymer Institute (DPI), PO Box 513, 5600 MB Eindhoven, The Netherlands
Fax: +31 40 247 4083; E-mail: u.s.schubert@tue.nl
[2] Unité de Chimie des Matériaux Inorganiques et Organiques (CMAT), Université catholique de Louvain, Place L. Pasteur 1, 1348 Louvain-la-Neuve, Belgium
[3] Center for NanoScience (CeNS), Ludwig-Maximilians-Universität München, Geschwister-Scholl Platz 1, 80333 München, Germany

Received: February 19, 2003; Revised: April 28, 2003; Accepted: June 13, 2003; DOI: 10.1002/macp.200350017

Keywords: graft copolymers; metal complex; micelles; supramolecular chemistry; terpyridine

Introduction

Nowadays, nanostructured materials have become a major field of research, in particular systems that are obtained by self-assembly processes. Prominent examples for such nanoobjects are micellar systems, which can be formed, e.g., from amphiphilic block copolymers. In a protic solvent an aggregation of the hydrophobic blocks takes place to form the micelle core, surrounded by a corona of the hydrophilic part that provides colloidal stability.[1] Micelles can be used in applications such as drug-delivery systems[2] or as templates for the synthesis of inorganic nanoparticles.[3] The block copolymer approach has recently been expanded from covalent to supramolecular block copolymers.[4] A variety of different blocks has been combined utilizing the formation of heteroleptic *bis*terpyridine ruthenium(II) complexes. Amphiphilic block copolymers based on PEG hydrophilic blocks and various hydrophobic blocks have been prepared utilizing the ruthenium(III)/(II) chemistry which allows the directed synthesis of AB-block copolymers. Subsequently, aqueous metallo-supramolecular micelles have been prepared and characterized.[5] In contrast to covalent copolymer micelles, the supramolecular micelles can be reversibly modified. An example is the removal of the corona through decomplexation with hydroxyethyl ethylenediaminetriacetic acid (HEEDTA) to obtain only the spherical core.[6]

A different architectural approach for amphiphilic materials is resembled by graft copolymers. So far, these materials have been synthesized by conventional covalent chemistry.

As an example, two methods have been applied to yield PMMA-*g*-PEG graft copolymers. The most popular reaction is a transesterification of a poly[(methyl methacrylate)-*co*-(isoheptyl methacrylate)] with a potassium alkoxide of a PEG.[7] Ten to fifteen grafts per 100 monomer units were obtained. Another approach to these materials is the copolymerization of methyl methacrylate (MMA) with a macromonomer consisting of a PEG bearing a methacrylate at one chain end.[8] In this specific case, micelles have not been reported so far. However, graft copolymers of different chemical composition have already been successfully used to prepare micelles.[9–13] Among the numerous examples previously reported are, for example, micelles obtained from graft copolymers containing inorganic (polyphosphazene[11], siloxane[12]) or natural (chitin[13]) blocks. The dependence of the micellar size to the degree of grafting has been investigated in some of these previous contributions. Indeed, the aggregation number has been observed to decrease with higher grafting degree.[8] In sharp contrast, a weak dependence of the micelle size on grafting density has been noted by other authors.[12]

In the present contribution, the synthesis and investigation of metallo-supramolecular aqueous micelles are reported, based on the recently described metallo-supramolecular PMMA-*g*-PEG graft copolymers.[14]

Experimental Part

Materials

The investigated graft copolymers **1a**–**c** have been prepared according to the route described in ref.[14] by reacting methoxy-poly(ethylene glycol) terpyridine ruthenium(III) trichloride[4] (PEG, $\bar{M}_n = 3000$) chains with poly(methyl methacrylate)s containing terpyridine groups as side chains. The coupling was performed by reduction of the metal center to ruthenium(II). The molecular weights and the average numbers of side chains are shown in Scheme 1 and Table 1.

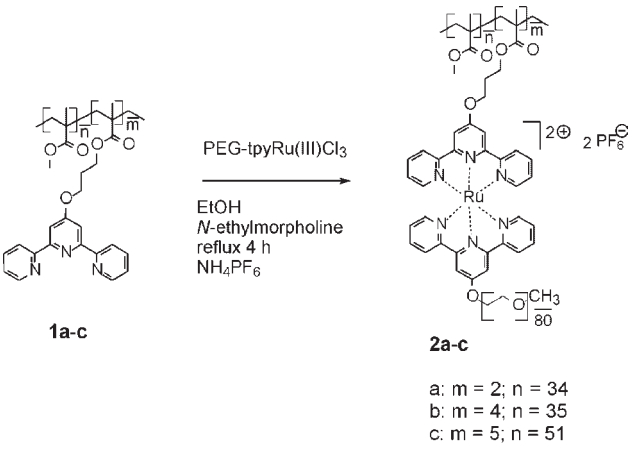

Scheme 1. Schematic representation of the graft copolymer synthesis.

Selected Analytical Data

1a

^{1}H NMR (400 MHz, $CHCl_3$): $\delta = 0.83$ (b, 30H, CH_3), 1.01 (b, 16H, CH_3), 1.80 and 1.89 (b, 30H, CH_2), 2.19 (m (b), 2H, CH_2), 3.61 (s, 56H, OCH_3), 4.19 (m (b), 2H, OCH_2), 4.33 (m (b), 2H, OCH_2), 7.40 (m, 2H, $H_{5,5''}$), 7.91 (ddd, 2H, $J = 8.06$, 2.20 Hz, $H_{4,4''}$), 7.98 (s, 2H, $H_{3',5'}$), 8.61 (d, 2H, $J = 8.06$ Hz, $H_{3,3''}$), 8.67 (d, 2H, $J = 5.86$ Hz, $H_{6,6''}$).

UV-vis (CH_3CN): λ_{max}/nm (ε/L · mol^{-1} · cm^{-1}) = 277 (39 200), 241 (42 900).

See also ref.[14]

1b

^{1}H NMR (400 MHz; $CDCl_3$): $\delta = 0.83$ (b, 30H, CH_3), 1.01 (b, 20H, CH_3), 1.80 and 1.89 (b, 32H, CH_2), 2.19 (m (b), 2H, CH_2), 3.61 (s, 48H, OCH_3), 4.19 (m (b), 2H, OCH_2), 4.33 (m (b), 2H, OCH_2), 7.40 (m, 2H, $H_{5,5''}$), 7.91 (ddd, 2H, $J = 8.06$, 8.06, 2.20 Hz, $H_{4,4''}$), 7.98 (s, 2H, $H_{3',5'}$), 8.61 (d, 2H, $J = 8.06$ Hz, $H_{3,3''}$), 8.67 (d, 2H, $J = 5.86$ Hz, $H_{6,6''}$).

UV-vis (CH_3CN): λ_{max}/nm (ε/L · mol^{-1} · cm^{-1}) = 278 (46 800), 249 (43 600).

See also ref.[15]

1c

^{1}H NMR (400 MHz; $CDCl_3$): $\delta = 0.83$ (b, 30H, CH_3), 1.01 (b, 20H, CH_3), 1.80 and 1.89 (b, 32H, CH_2), 2.19 (m (b), 2H, CH_2), 3.61 (s, 48H, OCH_3), 4.19 (m (b), 2H, OCH_2), 4.33 (m (b), 2H, OCH_2), 7.40 (m, 2H, $H_{5,5''}$), 7.91 (ddd, 2H, $J = 8.06$, 8.06, 2.20 Hz, $H_{4,4''}$), 7.98 (s, 2H, $H_{3',5'}$), 8.61 (d, 2H, $J = 8.06$ Hz, $H_{3,3''}$), 8.67 (d, 2H, $J = 5.86$ Hz, $H_{6,6''}$).

Table 1. Molecular characteristic features of the copolymers **1a**–**c**.

Copolymer	GPC data		Average degree of polymerization	Average number of terpyridine groups per chain[a)]
	$\bar{M}_n$ / g · mol^{-1}	PDI		
1a	3 700	1.61	36	2
1b	5 020	2.18	39	4
1c	6 800	1.89	56	5

[a)] Calculated from ^{1}H NMR data.

UV-vis (CH_3CN): λ_{max}/nm (ε/L · mol^{-1} · cm^{-1}) = 278 (46 200), 248 (43 300).

2a

^{1}H NMR (400 MHz, CD_3CN): $\delta = 0.81$ (b, 24H, alkyl, PMMA), 1.00 (b, 20H, alkyl, PMMA), 1.82, 1.90 (b, 26H, CH_2, PMMA), 3.33 (s, 3H, OCH_3, PEG), 3.52 (m, CH_3O-C$\underline{H}_2$C$\underline{H}_2$, PEG), 3.61 (s, 340H, OCH_3, PMMA, CH_2, PEG), 3.79 (m, 2H, CH_2, PEG), 3.91 (m, 2H, CH_2, PEG), 4.67 (m, 4H, OCH_2, C_3-alkylspacer), 7.18 (m, 4H, $H_{5,5''}$), 7.41 (m, 4H, $H_{6,6''}$), 7.92 (m, 4H, $H_{4,4''}$), 8.37 (2s, 4H, $H_{3',5'}$), 8.50 (m, 4H, $H_{3,3''}$).

UV-vis (CH_3CN): λ_{max}/nm (ε/L · mol^{-1} · cm^{-1}) = 242 (64 400), 268 (61 100), 304 (59 800), 485 (15 600).

See also ref.[14]

2b

^{1}H NMR (400 MHz, CD_3CN): $\delta = 0.80$ and 0.98 (b, 28H, alkyl, PMMA), 1.81 and 1.88 (b, 10H, CH_2, PMMA), 3.27 (s, 3H, OCH_3, PEG), 3.52 (m, $CH_3OC\underline{H}_2C\underline{H}_2$, PEG), 3.61 (s, 282H, OCH_3, PMMA, CH_2, PEG), 3.79 (m, 2H, CH_2, PEG), 3.91 (m, 2H, CH_2, PEG), 4.67 (m, 4H, OCH_2, C_3-alkylspacer), 7.18 (m, 4H, $H_{5,5''}$), 7.41 (m, 4H, $H_{6,6''}$), 7.92 (m, 4H, $H_{4,4''}$), 8.37 (2s, 4H, $H_{3',5'}$), 8.50 (m, 4H, $H_{3,3''}$).

UV-vis (CH_3CN): λ_{max}/nm (ε/L · mol^{-1} · cm^{-1}) = 242 (64 500), 268 (61 100), 304 (59 700), 485 (15 600).

2c

^{1}H NMR (400 MHz, CD_3CN): $\delta = 0.80$ and 0.98 (b, 29H, alkyl, PMMA), 1.81 and 1.88 (b, 10H, CH_2, PMMA), 3.27 (s, 3H, OCH_3, PEG), 3.52 (m, $CH_3OC\underline{H}_2C\underline{H}_2$, PEG), 3.61 (s, 282H, OCH_3, PMMA, CH_2, PEG), 3.79 (m, 2H, CH_2, PEG), 3.91 (m, 2H, CH_2, PEG), 4.67 (m, 4H, OCH_2, C_3-alkylspacer), 7.18 (m, 4H, $H_{5,5''}$), 7.41 (m, 4H, $H_{6,6''}$), 7.92 (m, 4H, $H_{4,4''}$), 8.37 (2s, 4H, $H_{3',5'}$), 8.50 (m, 4H, $H_{3,3''}$).

UV-vis (CH_3CN): λ_{max}/nm (ε/L · mol^{-1} · cm^{-1}) = 242 (64 400), 268 (61 200), 304 (59 300), 485 (15 700).

Instrumentation

Dynamic light scattering (DLS) measurements were performed on a Malvern 4700C apparatus equipped with a Malvern 7032 digital correlator and an Ion Laser Technology argon laser with a wavelength of 488 nm. A scattering angle of 90° was used for the measurements. The experimental correlation function was measured and analyzed with the CONTIN routine, which gives access to the distribution of hydrodynamic diameter (D_h). The measurements were repeated and analyzed at least ten times, in order to verify the reproducibility of the CONTIN analysis. The mean D_h was also calculated from the first cumulant of a cumulant expansion of the correlation function, using the Stokes-Einstein approximation, as described elsewhere.[16]

Transmission electron microscopy (TEM) observations have been carried out using a JEOL 2000 FX microscope operating at a voltage of 200 kV. Samples were prepared by drop-casting the aqueous micellar solution onto a Formvar-coated copper TEM grid and directly observed without any further contrasting (sample **2a**,**b**), or contrasted with phosphotungstic acid (sample **2c**).

Atomic force microscopy (AFM) images were obtained either on a NT-MDT Smena-B or a Digital Instruments Nanoscope IIIa Multimode AFM-apparatus. Micelles were deposited on a silicon wafer by spin-coating on the plate, and measured with the Multimode operated in air utilizing the Tapping Mode. Furthermore, direct imaging in aqueous solution was performed on a NT-MDT Smena-B, equipped with a solution-imaging head (DI Nanoprobe silicon nitride tip). The sample was deposited on a mica substrate and measured directly after the setup of the device (ca. 5 min).

Preparation of the Micelles

The metallo-supramolecular graft copolymers as obtained from the synthesis are poorly soluble in water. Therefore, each copolymer was dissolved in *N*,*N*-dimethylformamide (DMF) with a concentration of 1 g · L^{-1}. Then water was added stepwise by increments of 50 μL under vigorous stirring and the scattered intensity of the resulting solution was measured. At a critical concentration of added water, aggregation of the water-insoluble PMMA block is observed, which resulted in an important increase of scattered intensity. The so-called critical water concentration (cwc) was accordingly measured as defined by Eisenberg et al. in ref.[17] Subsequently, the DMF/water solution was dialyzed several times against water (Spectra-Por dialysis bags, cut-off 6 000–8 000 Da). The final concentration of the copolymer in pure water was set to 0.5 g · L^{-1}.

Results and Discussion

Recently, it has been shown that the coupling of terpyridine-functionalized polymers via complexation with ruthenium(II) ions represents a powerful tool for the engineering of block[4] as well as graft copolymers.[14] Utilizing the directed synthesis of asymmetric terpyridine ruthenium(II) complexes via an intermediate Ru^{III} *mono*complex, the combination of hydrophilic PEG blocks with hydrophobic polymers such as polystyrene or poly(ethylene-*co*-butylene) leads to a variety of amphiphilic block copolymers. Furthermore, these materials could be used for the formation of aqueous micelles. Recently, the concept of supramolecular polymers based on ruthenium(II)-terpyridine complexes has been extended to graft copolymer architectures.[14] In this case amphiphilic systems, consisting of PEG chains grafted to a PMMA backbone, have been obtained, which are expected to show a similar behavior concerning the formation of micelles (Scheme 2). In order to explore this possibility, three graft copolymers with different degree of grafting (amount of side chains) have been synthesized according to a recently described procedure (ref.[14]) and investigated regarding their micellization behavior. In these three samples, the length of the PEG side chains was kept constant while the length of the PMMA

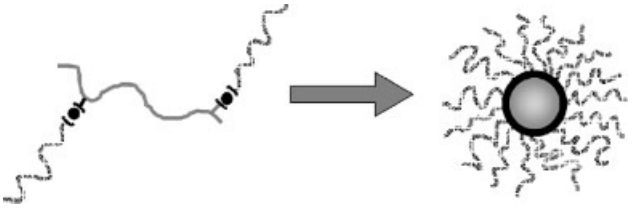

Scheme 2. Schematic representation of the micelle formation.

backbone was varied (Scheme 1 and Table 1). The PEG chains were synthesized by living anionic polymerization and have a narrow polydispersity index while the PMMA backbones were prepared by free radical polymerization and are therefore characterized by a rather broad polydispersity index (Table 1). In order to link the PEG chains to the backbone, they were first converted into a ruthenium(III) *mono*complex by complexing the free terpyridine end with $RuCl_3$.[4] The grafting procedure (Scheme 1) was performed by refluxing the *mono*complex with the PMMAs bearing the free terpyridines (**1a**–**c**) under reductive conditions (ethanol with a catalytic amount of *N*-ethylmorpholine). Exchange of the counterions and preparative size exclusion chromatography (BioBeads SX1) led to pure products. Since the graft copolymers were not readily soluble in water, pure water was added dropwise to a solution of the graft copolymers in DMF and the obtained solution was dialyzed against water, leading to frozen micelles. Details about this method can be found elsewhere.[18] Briefly, the graft copolymer chains are completely solvated in the initial DMF solution. As the added water content increases, the solvent quality for the PMMA backbone decreases progressively. At a critical water content, aggregation takes place. However, the structure of the accordingly formed aggregates is still labile. At higher added water content, the solubility and chain mobility of the PMMA chains is decreased and the kinetic process of polymer self-assembly and structural rearrangment of the aggregates can be very slow. After dialysis and elimination of DMF, the system is completely frozen. These systems are generally considered to be out of equilibrium since the kinetic process of aggregate rearrangment in the DMF/water mixture is difficult to control. The UV-spectra of the samples in DMF and in water revealed no significant changes in the shape and intensity of the absorption bands (Figure 1), suggesting that the integrity of the graft copolymers is maintained during micelle preparation.

Light scattering (LS) was used as a tool to characterize the aqueous micelles formed by the three investigated graft copolymers. In a first experiment, the scattered intensity (I) was recorded as a function of the amount of added water in order to determine the critical water concentration (cwc, see experimental part). Because of the preparation method used, it is meaningless to define a critical micelle concentration (cmc). It is, however, possible to extract information from the cwc. Because the cwc is strongly sensitive to the initial concentration of the copolymer in DMF,[17] the three

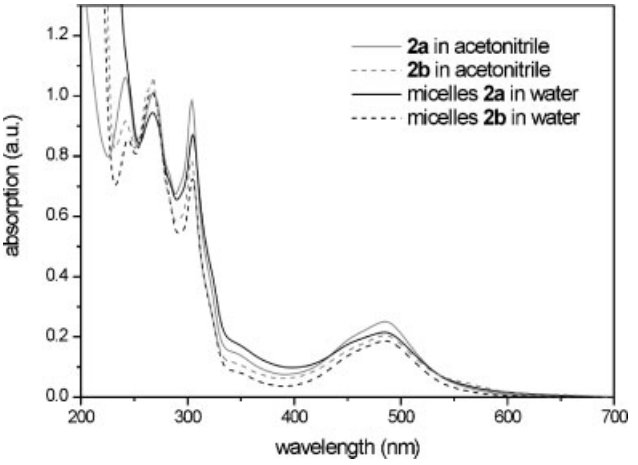

Figure 1. UV-Vis spectrum of samples **2a** and **2b** dissolved as unimers in acetonitrile and aggregated into micelles in water.

investigated copolymers were dissolved at the same concentration in DMF, in order to make a comparison possible. The three curves shown in Figure 2 have a sigmoidal shape. At low added water content, I is low because the graft copolymer chains exist as unimers. Then, an increase in I is observed because of the formation of aggregates, as proven by the observation of a correlation function. Finally, I reaches a plateau value, as an indication that the aggregates are already frozen at these water contents and do not further modify their structure. The cwc has been found to be in the same range for the three investigated graft copolymers (400–600 μL). It should, however, be noted that the cwc was lowest for the **2a** sample, in agreement with a lower wt.-% of hydrophilic PEG blocks in this graft copolymer.

Dynamic light scattering (DLS) was then used in order to determine the characteristic size of the accordingly formed

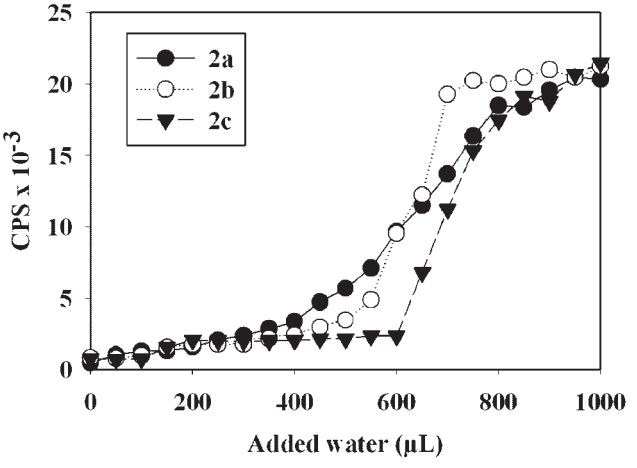

Figure 2. Scattered light intensity (I, counts per second CPS) as a function of the added water amount for the graft copolymers **2a**, **2b**, and **2c** initially dissolved in DMF at a concentration of $1\ g \cdot L^{-1}$.

micellar objects. The DLS results were analyzed by several methods: The first cumulant of a cumulant expansion led to the mean hydrodynamic diameter (D_h) and the CONTIN routine allowed the distribution of hydrodynamic diameters to be calculated. The mean D_h calculated directly from the experimental correlation function is too large to fit to classical block copolymer micelles. Utilizing an analysis of the experimental correlation function by the CONTIN routine systematically showed two populations for the **2a** and **2b** samples, while only a single broad population was observed for **2c** (Figure 3). The reproducibility of these results was checked, in order to eliminate any calculation artefact arising from the CONTIN routine. Moreover, dilution of the sample did not modify the characteristic sizes as measured by DLS, in agreement with the formation of frozen micelles. In analogy with previously reported results on micelles formed by metallo-supramolecular linear block copolymers,[5,6,18] the two populations were attributed to micelles (and small aggregates of micelles) and large aggregates of micelles. However, in contrast to the results obtained from the linear supramolecular block copolymers, the polydispersity associated to each type of species was very large in the present case. Filtration of the samples (syringe filters with a porosity of 450 nm) resulted in a shift of the large aggregates population to smaller sizes, suggesting that the shearing effect induced by the filtration procedure partly disrupted the large aggregates.

The polydispersity found in the DLS results could originate from two factors: (i) the polydispersity of the primary micelles is broad resulting in broad aggregates (ii) the polydispersity of the primary micelles is narrow but a continuum of aggregates is formed. DLS is not the appropriate tool to use for gaining deeper information on the system. For that purpose, transmission electron microscopy (TEM) and atomic force microscopy (AFM) have been utilized for a more detailed investigation of the morphology.

TEM was first carried out directly on micelles dried on a formvar-coated copper grid. The results are shown in Figure 4 for samples **2a** and **2b**. Although no contrasting agent had been used, spherical micelles are seen in these pictures. The micelles appear as white spheres surrounded by a dark ring. The dark ring could be tentatively attributed to the presence of strongly electron adsorbing ruthenium ions found in the metallo-supramolecular complexes. The micelles are polydisperse in size but all have a spherical shape. The dark rings are not clear-cut, suggesting that the interface between the PMMA core and the PEG corona of the micelles is not sharp. The average size of these micelles lies in the 15–20 nm range and no clear difference can be seen between the micelles formed by sample **2a** and **2b**, because of the large size polydispersity. In the case of **2c**, the TEM results did not allow an identification of the structural features. The dark rings were very diffuse (data not shown because it is too blurry) and the mean size of the objects seemed to be larger than for samples **2a** and **2b**. In order to obtain more information, micelles from sample **2c** were negatively stained with phosphotungstic acid (Figure 5). This staining procedure leads to a dark background on which the micelles are observed as white spots. The TEM picture of Figure 5 clearly shows that very polydisperse

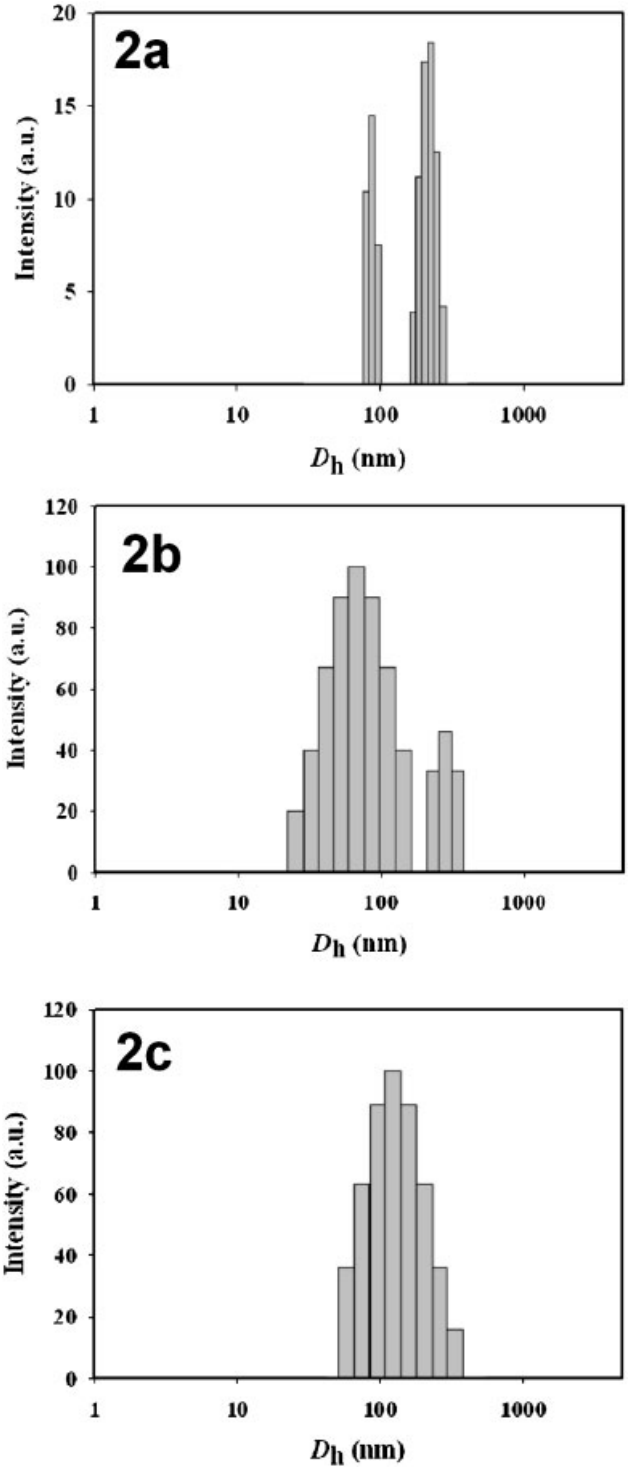

Figure 3. CONTIN size distribution histogram measured on aqueous micelles from **2a**, **2b**, and **2c**.

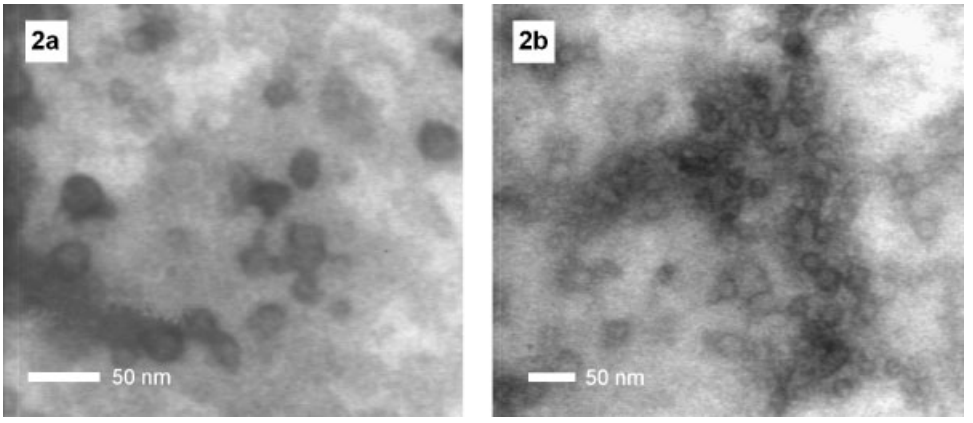

Figure 4. TEM images of micelles from **2a** and **2b** observed without contrasting.

spherical micelles with an average size of approx. 25–40 nm are formed in the case of sample **2c**.

Subsequently, AFM investigations were performed to confirm the TEM results. First, AFM measurements were performed on micelles spin-coated on a silicon wafer and therefore observed in the dried state. This is illustrated in Figure 6 for the sample **2a**. Polydisperse spherical micelles were observed on the substrate. Considering the tip convolution effect, the lateral size of these objects was in agreement with the TEM pictures. The height of these micelles was around 5 nm. This small size can be explained by the collapse of coronal PEG chains on the PMMA core during the drying process. In this respect, the height of the micelles should be close to the diameter of the PMMA core of the micelles. Since drying can deeply affect micellar morphology, micelles from sample **2a**–**c** were also directly imaged under water by AFM. The results are shown in Figure 7, in which the inserts are high magnification pictures. A dense layer of micelles on the surface was observed in each case. This could explain the significant decrease of the tip-convolution effects. The micelles are spherical and a broad polydispersity is again observed. The lateral sizes are in agreement with the previous TEM and AFM observations. The height contrast revealed characteristic sizes in the 5 nm range, which is in agreement with the size of the PMMA core. This suggests that the AFM tip can more or less penetrate into the hydrated PEG corona and hits the PMMA core. The characteristic dimensions measured by TEM and AFM for the three investigated samples are summarized in Table 2. Although the studied samples were characterized by different molecular parameters, their self-association is leading to rather similar types of micelles. The similarity of the results is obvious for samples **2a** and **2b**, while sample **2c** is different from the two others. However, because of the large polydispersity of the micelles, it is impossible to draw a clear trend.

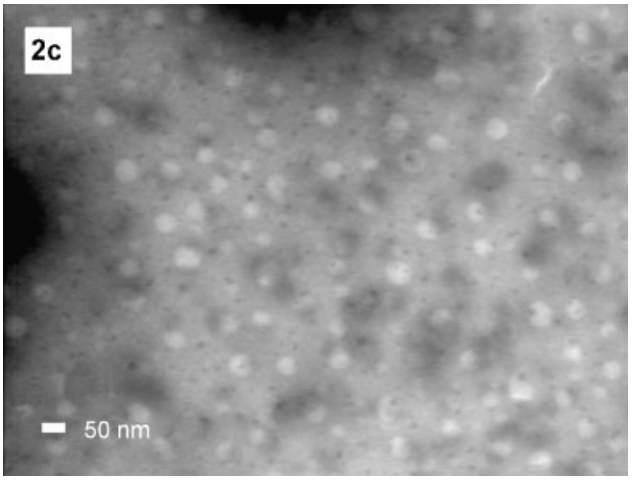

Figure 5. TEM image of micelles from **2c** (negative contrasting with $H_3PO_4 \cdot 12WO_3$).

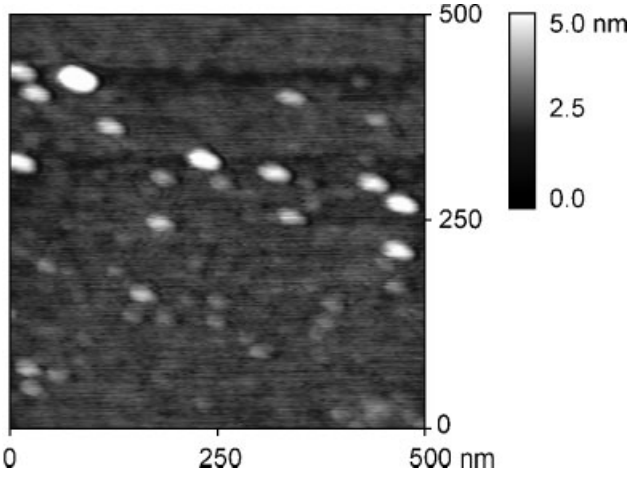

Figure 6. AFM image (height) of dried micelles from **2a**, spin-coated on a silicon wafer.

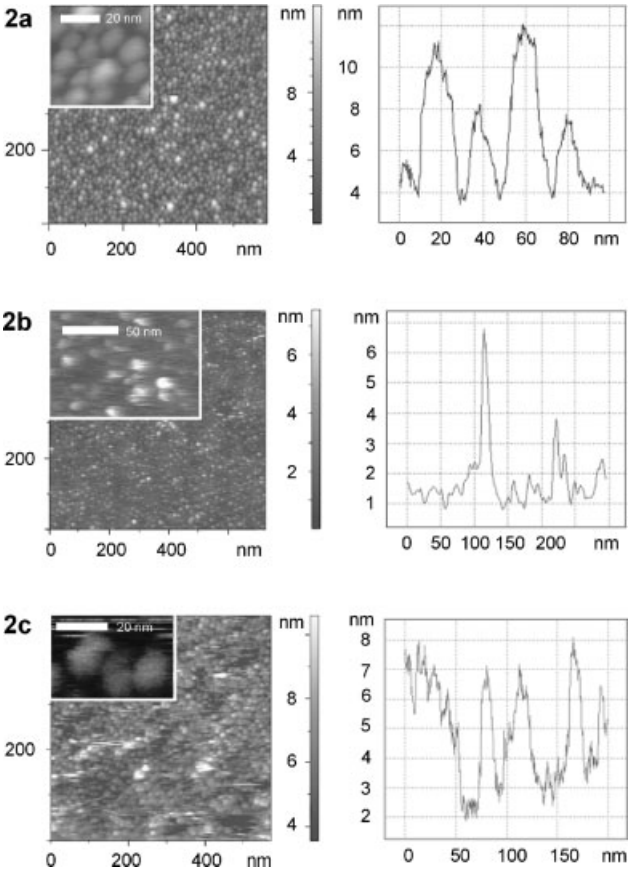

Figure 7. AFM images (height) and cross section of micelles from **2a**–**c** measured in aqueous solution.

Table 2. Characteristic dimensions (nm) of aqueous micelles formed by compounds **2a**–**c**, as determined by AFM in water, TEM, and DLS (D_{xy}: lateral dimension of the micelles as measured by AFM or by TEM; D_z: height of the micelles as measured by AFM; D_h (CONTIN) is the mean size of the small size population).

Sample	PEG	AFM		DLS		TEM
	wt.-%	D_{xy}	D_z	D_h (CONTIN)	D_h (mean)	D_{xy}
2a	62	≈15	≈5–7	79	165	≈15–20
2b	71	≈15	≈5–7	67	110	≈15–20
2c	69	≈25	≈6–8	123	188	≈25–40

Conclusions

Amphiphilic metallo-supramolecular graft copolymers have been synthesized and investigated, which differ from the average number of grafted PEG blocks and the length of the PMMA backbone. Subsequently, aqueous micelles have been prepared and analyzed by DLS, TEM, and AFM. Polydisperse spherical micelles that are clustering into larger structures were observed. A good correlation was found between TEM and AFM measurements. These results are in agreement with previous investigations on aqueous micelles formed by linear metallo-supramolecular block copolymers. However, the polydispersity of the primary micelles is much larger than for these previously investigated samples. This is thought to result from the polydispersity of the samples both in the PMMA chain length and in the distribution of the grafted PEG along the PMMA backbone. Although they have different compositions, no clear difference was observed between the micelles formed by the three investigated samples. Further studies will include the synthesis of graft copolymers with different lengths of the main and the side chains and the application of controlled polymerization techniques.

Acknowledgement: This study was supported by the *Deutsche Forschungsgemeinschaft* (SFB 486), the *Fonds der Chemischen Industrie* and the *Dutch Polymer Institute* (DPI). JFG is grateful to the *FNRS* for a Chargé de Recherches fellowship and to the *ESF SUPERNET Programme*.

[1] I. W. Hamley, "*The Physics of Block Copolymers*", Oxford University Press, Oxford 1998.
[2] M. Yokoyama, T. Okano, Y. Sakurai, H. Ekimoto, C. Shibazaki, K. Kataoka, *Cancer Res.* **1991**, *51*, 3329.
[3] S. Förster, M. Antonietti, *Adv. Mater.* **1998**, *3*, 195.
[4] B. G. G. Lohmeijer, U. S. Schubert, *Angew. Chem.* **2002**, *114*, 3980; *Angew. Chem., Int. Ed.* **2002**, *41*, 3825.
[5] J.-F. Gohy, B. G. G. Lohmeijer, U. S. Schubert, *Macromolecules* **2002**, *35*, 4560.
[6] J.-F. Gohy, B. G. G. Lohmeijer, U. S. Schubert, *Macromol. Rapid Commun.* **2002**, *23*, 555.
[7] M. A. Twaik, M. Tahan, A. Zilka, *J. Polym. Sci., Part A: Polym. Chem.* **1969**, *7*, 2469.
[8] G. Bo, B. Wesslén, K. B. Wesslén, *J. Polym. Sci., Part A: Polym. Chem.* **1992**, *30*, 1799.
[9] I. Berlinova, A. Anzil, I. Panaiotov, *J. Macromol. Sci. Chem.* **1992**, *29*, 975.
[10] Y. Ma, T. Cao, S. E. Webber, *Macromolecules* **1998**, *31*, 1773.
[11] J. Y. Chang, P. J. Park, M. J. Han, *Macromolecules* **2000**, *33*, 321.
[12] Y. Lin, P. Alexandridis, *J. Phys. Chem. B* **2002**, *106*, 10845.
[13] K. Aoi, A. Takasu, M. Okada, T. Imae, *Macromol. Chem. Phys.* **1999**, *200*, 1112.
[14] U. S. Schubert, H. Hofmeier, *Macromol. Rapid Commun.* **2002**, *23*, 561.
[15] H. Hofmeier, U. S. Schubert, *Macromol. Chem. Phys.* **2003**, *204*, 1391.
[16] P. Stepanek, in: "*Dynamic Light Scattering*", W. Brown, Ed., Oxford University Press, London 1972.
[17] L. Zhang, H. Shen, A. Eisenberg, *Macromolecules* **1997**, *30*, 1001.
[18] [18a] J.-F. Gohy, B. G. G. Lohmeijer, S. K. Varshney, U. S. Schubert, *Macromolecules* **2002**, *35*, 7427; [18b] J.-F. Gohy, B. G. G. Lohmeijer, S. K. Varshney, B. Décamps, E. Leroy, S. Boileau, U. S. Schubert, *Macromolecules* **2002**, *35*, 9748.

